



Table 1 The formulations of RDX-*HTPB* propellants

	HTPB	RDX-0	RDX-1	RDX-6
RP-0	25wt%	75wt%		
RP-1	25wt%		75wt%	
RP-6	25wt%			75wt%

RP: RDX-*HTPB* propellants

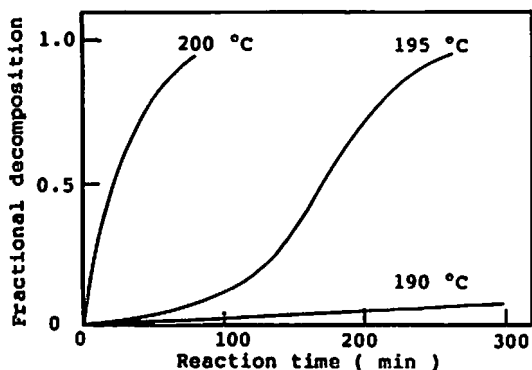


Fig. 1 Representative isothermal decomposition of RDX without milling at various temperatures

is then hermetically sealed with an aluminum cover having a pinhole at the center. The crucible has a 4 mm inside diameter and is 2.5 mm in height.

The pin-holed aluminum crucible was used in order to repress sublimation and evaporation of the RDX. The diameter of the pinhole was  $0.05 \pm 0.002$  mm. As preliminary experiments, an amount of sublimed or evaporated RDX which was directly trapped just above the crucible was determined by the quantitative analysis. A weight decrease caused by sublimation or evaporation of RDX was within  $\pm 5\%$ .

### 2.3 Measurement of linear burning rate

Strands for the linear burning rate measurement were formed in a 6mm x 6mm x 60mm shape. Time needed for the 40 mm burning of the strand piece was measured by means of a chimney type strand burner under pressurized nitrogen ranging from 30 to 70  $\text{kgf/cm}^2$ .

## 3. Results and discussion

### 3.1 Isothermal decomposition of simple RDX

Fig. 1 shows the results of an isothermal decomposition of RDX-0. Fractional decomposition ( $x$ ) vs. reaction time ( $t$ ) curves ( $x$ - $t$  curves, hereafter) for RDX-0 have two different characteristic features based on

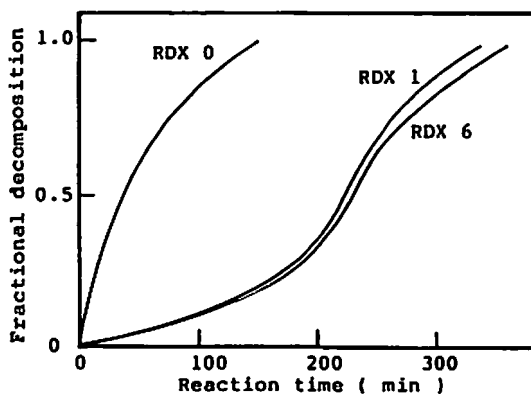


Fig. 2 Effect of milling on the isothermal decomposition of RDX at 200 °C

reaction temperature. One is the isothermal decomposition above 200 °C which has an upward convex shape of the  $x$ - $t$  curves. The other is the isothermal decomposition under 195 °C which has a sigmoidal shape and shows a large temperature dependence. A difference in the shape of the decomposition curves indicates that the thermal decomposition proceeded according to different mechanisms depending upon the reaction temperature. SEM observations of the samples which are quenched during decomposition showed that the decomposition above 200 °C proceeded in a molten phase, while the decomposition under 195 °C proceeded in a solid phase.

The thermal decomposition of simple RDX was affected by its particle size. Fig.2 shows the effect of milling on the isothermal decomposition of RDX at 200 °C. RDX without milling had an upward convex shape of its  $x$ - $t$  curve and a large decomposition rate compared with milled RDX. On the other hand, the  $x$ - $t$  curve of the milled RDX had sigmoidal shape and its decomposition rate was smaller. Of course, milled RDX also showed a thermal decomposition in both the molton and solid phase according to the decomposition temperature.

Fig. 3 shows the results of the isothermal decomposition of RDX-6 in the temperature range from 215 °C to 200 °C. As previously stated,  $x$ - $t$  curves are convex upwards indicating that the decomposition rate decreases linearly with the reaction time. Applicability to first order rate equation (1) for the results is shown in Fig. 4

$$\ln(1-x) = -kt \quad (1)$$

where  $x$  is the fractional decomposition,  $t$  is the reac

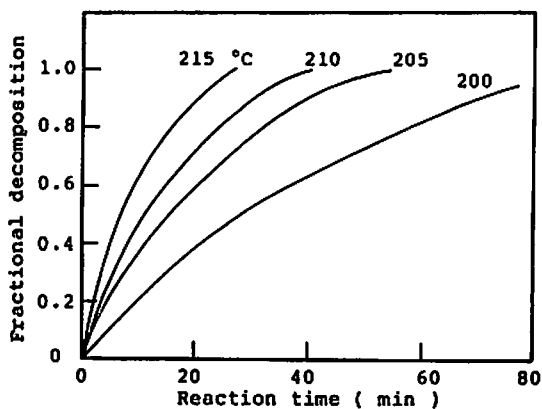


Fig. 3 Isothermal decomposition of milled RDX for 6 hours

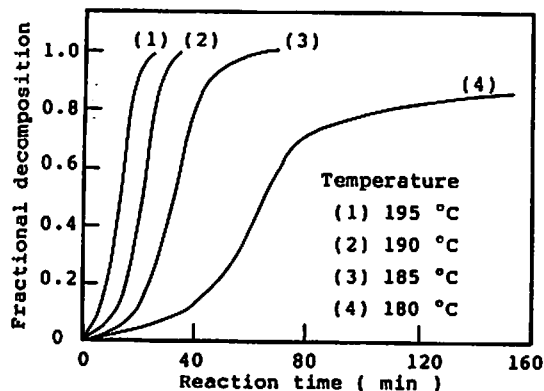


Fig. 5 Isothermal decomposition of RDX-HTPB propellants which contain RDX without milling

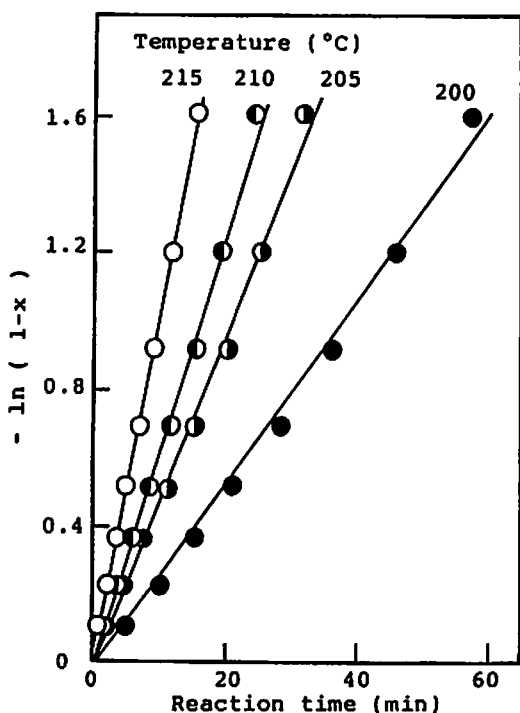


Fig. 4 First order plots for the isothermal decomposition of milled RDX for 6 hours

tion time and  $k$  is the constant of reaction system. Fig. 4 shows good straight lines and the rate constants of the decomposition were obtained from the slope for these lines. Activation energies for the molten phase decomposition of RDX were calculated as 146 kJ/mol for RDX-0, 170 kJ/mol for RDX-1 and 196 kJ/mol for RDX-6 from the Arrhenius plots of the rate constants.

Oyumi<sup>5)</sup> reported a first order rate equation and the activation energy 200 kJ/mol for the molten phase decomposition by using an open aluminum crucible. Miller et al.<sup>6)</sup> also reported the same rate equation and 213 kJ/mol by using the RDX sample prepared as thin films under pressurized conditions below 2.0 GPa over the temperature range from 205 °C to 235 °C. The present study gave the same rate equation and somewhat smaller activation energies for the molten phase decomposition of RDX.

The low temperature decomposition of simple RDX in Fig. 1 had a sigmoidal shape of the  $x-t$  curves and the temperature dependence of the reaction rate was very large as previously stated. Furthermore, the induction period of RDX (especially without milling) decomposition were different with each run even though the overall time of the reaction was almost same. This indicates that nucleation on the RDX surface without milling for the decomposition occurred at random because of the cleanliness of its surface.

### 3.2 Isothermal decomposition of RDX propellants

Fig. 5 shows the thermal decomposition of RDX propellants RP-0 which contained RDX-0 in the temperature range from 180 °C to 195 °C.

From these results, the thermal decomposition of RDX propellants proceeded at a relatively low temperature compared with that of simple RDX. That is, the decomposition rate depended on the particle size of the RDX and the larger the particle size, the lower the decomposition temperature. This is interpreted as the thermal effect on the reaction rate. That

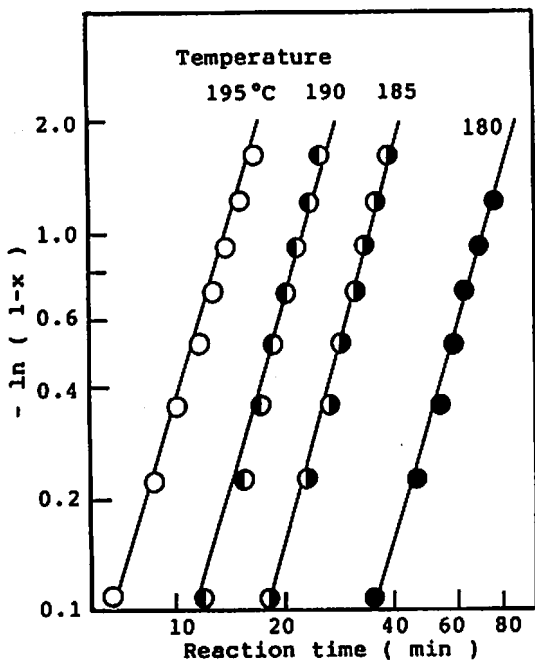


Fig. 6 Avrami-Erofeev plots for the isothermal decomposition of RDX-HTPB propellant which contains RDX without milling

is, when the thermal decomposition occurs on the RDX particle surface, a heat flux released to the atmosphere depends on its surface area. Accordingly, a large RDX particle acquires a high heat accumulation because of its small specific surface area having a high thermal decomposition rate.

SEM observations of the quenched sample during decomposition showed that the decomposition of propellant proceeded in the solid phase. Also,  $x-t$  curves for RDX propellant had a sigmoidal shape similar to that of the decomposition of a simple RDX at low temperatures where the reaction proceeds in the solid phase. These results suggest that the thermal decomposition of both the simple RDX at low temperatures and RDX propellant would proceed according to the same reaction mechanism.

The Avrami-Erofeev equation described by Eq. (2) agreed well with the sigmoidal curves which corresponded to the phenomena accompanied by phase transformation such as melting<sup>7</sup>.

$$1-x = \exp(-Bt^k) \quad (2)$$

where  $x$  is the fractional decomposition,  $t$  is the reaction time,  $B$  is the constant depending on the temperature,  $k$  is the constant of the reaction system.

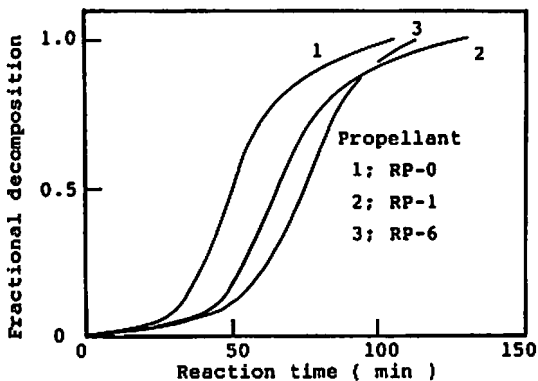


Fig. 7 Effect of milling on the isothermal decomposition of RDX-HTPB at 180°C

Avrami-Erofeev plots of the results in Fig. 5 corresponded well with this equation (Fig. 6). Activation energies obtained from the constant  $B$  gave the value of 154 kJ/mol for the RDX-0 propellant, 153 kJ/mol for the RDX-1 propellant and 152 kJ/mol for the RDX-6 propellant<sup>8</sup>.

The thermal decomposition of RDX-HTPB propellants was also affected by the particle size of RDX contained. Fig. 7 shows the effect of milling on the isothermal decomposition of the RDX-HTPB propellants at 180°C. RDX-HTPB propellants irrespective as to whether the contained RDX was milled or not had sigmoidal  $x-t$  curves which were obtained in the case of the low temperature decomposition of simple RDX. Furthermore, the propellant which contained RDX without milling had a larger decomposition rate similar to the isothermal decomposition of simple RDX.

### 3.3 Burning characteristics of RDX propellants

Linear burning rates of RDX propellants under pressurized conditions are shown in Fig. 8. Linear burning rates increased with pressure and obeyed Vieille's equation (3).

$$V = BP^n \quad (3)$$

where  $V$  is the linear burning rate,  $B$  is the constant,  $P$  is the pressure and  $n$  is the pressure exponent. Pressure exponents are 0.45 for the propellant RP-0, 0.44 for RP-1 and 0.52 for RP-6.

Contrary to the thermal decomposition of RDX propellants, the propellant which contains smaller RDX particles has a larger linear burning rate over all pressure ranges. This indicates that in the RDX-HTPB propellant combustion the condensed phase

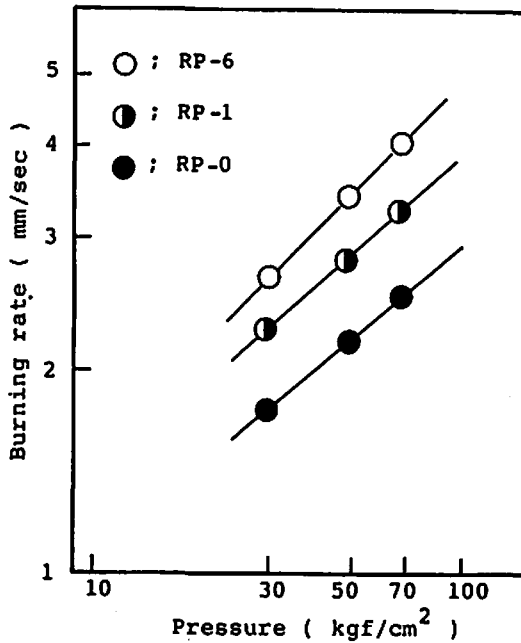


Fig. 8 Effect of milling of RDX on the linear burning rates of RDX-HTPB strands

decomposition of RDX does not play an important role to determine the burning rate compared with the other steps such as the decomposition of binder or some gas phase reactions. This is ascribed to the high activity of the condensed phase decomposition of RDX.

#### 4. Conclusions

The thermal decomposition of both simple RDX and RDX-HTPB propellants and the combustion of RDX-HTPB propellants were examined using pulverized RDX. The following results were obtained.

(1) The mechanism of the thermal decomposition of simple RDX was different with reaction temperature.

That is, the isothermal decomposition above 200 °C proceeded in the liquid phase obeying the first order rate equation. On the other hand, the isothermal decomposition under 195 °C occurred in the solid phase obeying the Avrami-Erofeev equation.

(2) The thermal decomposition of RDX-HTPB propellant proceeded in the solid phase obeying the Avrami-Erofeev equation, which was similar to the low temperature decomposition of simple RDX.

(3) The isothermal decomposition of both simple RDX and its propellant were affected by pulverization, and RDX with a larger particle size had a large thermal decomposition rate.

(4) Contrary to the thermal decomposition of RDX propellants, the propellant which contains smaller RDX particles has a larger linear burning rate over all the pressure ranges.

#### References

- 1) Boggs, T. L., "Prog. Astronaut. Aeronaut. 90", 1211-175 (1984)
- 2) Oyumi, Y. and T. B. Brill, *Combust. Flame*, 62, 213 (1985)
- 3) Shackelford, S. A., M. B. Coolidge, B. B. Goshgarian, B. A. Loving, R. N. Rogers, J. L. Janney, and M. H. Ebinger, *J. Phys. Chem.*, 89, 3118 (1985)
- 4) Zhao, X., T. B. Hints and Y. T. Lee, *J. Chem. Phys.*, 88, 801 (1988)
- 5) Oyumi, Y., *Propellants Explos.*, 13, 42 (1988)
- 6) Miller, P. J., S. Block and G. J. Piermarini, *Combust. Flame.*, 83, 174 (1991)
- 7) Avrami, M., *J. Chem. Phys.*, 7, 1103 (1939) ; 8, 212(1940) ; 9, 177 (1941)
- 8) Nakamori, I., H. Nakamura, T. Hayano and S. Kagawa, *Bull. Chem. Soc. Japan*, 47, 1827 (1974)

## RDXおよびRDX-HTPB固体推進薬の熱的挙動

中村英嗣\*, 中下吾郎\*\*, 加藤一成\*\*, 原 泰毅\*

RDXのみおよびRDX-HTPB系固体推進薬の熱反応および熱焼反応の機構を粉碎したRDXを用いて検討し, 以下の結果が得られた。

RDXのみの200℃以上での等温熱分解反応は熔融状態で, 一次反応速度式に従って進行する。一方, 195℃以下のRDXのみおよびRDX-HTPB系固体推進薬の熱分解反応は固体状態で, Avrami-Erofeevの式に従って進行する。

RDXのみおよびRDX-HTPB系固体推進薬の熱分解反応は粉碎の影響を受け, 粉碎したRDX粒子の粒子径が大きくなれば大きくなるという特異な結果を示した。しかし, 粉碎したRDXを用いて調製した固体推進薬の線燃焼速度は, これらの熱分解反応とは逆に, 測定したいずれの圧力下でもRDX粒子の粒子径が小さくなれば大きくなるという結果を示した。

(\*九州工業大学工学部応用化学教室 〒804 北九州市戸畑区仙水町 1-1

TEL 093-871-1931 (Ext 447) FAX 093-881-3418

\*\*日本油脂(株)愛知事業所 武豊工場 研究開発部SRグループ 〒470-23

愛知県知多郡武豊町字北小松谷 61-1 TEL 0569-72-1954

FAX 0569-73-7376)